Int. J. Multiphase Flow, Vol. 1, pp. 771–791. Pergamon/Elsevier, 1975. Printed in Great Britain.

DRYOUT IN SERPENTINE EVAPORATORS

S. A. FISHER and S. K. W. YU

Central Electricity Research Laboratories, Kelvin Avenue, Leatherhead, Surrey, England

(*Received* 5 *January* 1974)

Abstract—Waterside on-load corrosion failures in power station evaporators have resulted from dryout along the upper surfaces of the tubes in serpentine arrangements.

It is shown that this type of dryout can occur at intermediate qualities over a wide range of flow rates and pressures for heat fluxes much less than in vertical tubes.

A type of flow which is here called "surge flow" has been identified as being particularly likely to lead to dryout, because the top surfaces are wetted only intermittently by waves or plugs of frothy liquid.

A method is being developed for assessing the likelihood of dryout under surge flow conditions. It correctly predicts the dryout boundaries in a pressurized steam/water facility.

1. INTRODUCTION

There has now been extensive operating experience of dryout causing on-load corrosion failures in power station evaporators. These have covered low, intermediate and high qualities over a wide range of pressures, flow rates and heat fluxes. In most cases, the recommended chemical treatment was being applied.

One of the earliest cases was in the evaporators at Trawsfynydd power station where a number of tube failures occurred during the first few months of operation (Lunn & Harvey 1970). The maximum heat fluxes were considerably less than the heat fluxes generally observed for burnout in vertical tubes and failure was not caused by overheating but by waterside on-load corrosion. The corrosion patterns were very distinctive and suggested that the upper surfaces had been drying out. This was later confirmed by work carried out under contract at Heat Wrightson Ltd. (Lis & Strickland 1970) on a pressurized steam/water loop. It was shown that permanent dry patches would have occurred in the station evaporators where corrosion failures were found. Attempts to resolve the problem by chemical treatment were only partially effective and it was not until the water flow rate was increased as recommended by Lis to avoid dryout that further failures were prevented.

It seems clear that dryout results in a local concentration of aggressive chemicals but there are a number of factors determining the levels of concentration (Garnsey, Hearn & Mann 1972), and it is not a simple matter to determine reliable quantitative estimates, or to establish in advance the full implications of any particular chemical treatment. For example, there has been little history of corrosion in the final dryout zones of once-through boilers even though this might be expected from the chemistry at the dryout boundary. A proper physical description of this boundary is lacking here and this is important for it will be a very ill-defined diffusive type of dryout, even under stable operating

conditions. The corrosion will be spread out and therefore perhaps tolerable unlike the highly localized biting attack resulting from more stable dry patches.

It will clearly not be a simple matter to establish the precise details of each and every type of dryout and for the time being any conditions leading to dryout in evaporators (perhaps other than the final dryout in a once-through system) should be regarded as highly undesirable. It is important to determine what these might be and this paper describes some of the work that has been carried out to investigate them in serpentine evaporators.

At the time of the Trawsfynydd problem there was speculation that dryout might disappear at the higher pressures of current plant (18 MN/m^2), mainly based on the intuitive reasoning that the greatly reduced liquid/vapour ratio (~ 4) would be less likely to give rise to phase separation. The first need was to investigate this possibility. A high pressure steam/water system was not available and so the C.E.R.L. Freon 12 facility was used. As will be shown in Section 2, not only was dryout shown to occur but it appeared to be more likely at higher pressures.

These problems had to be taken very seriously and as well as looking at the systems of immediate interest on high pressure steam/water facilities, a broad based study was instigated aimed at more general application (Section 3). The geometries and operating conditions of nuclear power station evaporators vary so widely that it is particularly important to come to a proper understanding of the physical mechanisms involved. As well as the Freon 12 system, therefore, air/water and atmospheric steam/water facilities have been used to enable flow visualization techniques to identify the types of flow responsible for dryout in the Trawsfynydd situation (Section 3.1). These types of flow have been investigated in some detail, using liquid film thickness probes (Section 3.2), and a predictive method for assessing dryout is being developed (Section 3.3).

2. FREON 12 TESTS

2.1 *Freon modelling*

The use of Freon 12 to simulate high pressure steam/water is becoming a common practice. A whole range of Freons have been produced commercially, initially for refrigeration purposes, but recently in increasing quantities for aerosol propellants. They can break down under heat to very posionous products but normally are non-toxic, odourless and present few problems to personnel.

Freon 12 was chosen for a number of reasons not least that most of its physical and thermodynamic properties are well tabulated. The low boiling point ensures that it is a vapour at atmospheric pressure and tests can be carried out up to the critical point for temperatures only a little exceeding that of ordinary boiling water. The low latent heat helps considerably by reducing the heat fluxes that are needed for steam/water by roughly seven times. The resulting low heat fluxes are much less likely to damage test sections during dryout.

Most of the work on modelling has been carried out on other geometries and no scaling laws for general application have been established for horizontal tubes. Rather than attempt to determine precise scaling laws of our own, which would have required a very extensive series of tests in steam/water as well as in Freon 12, it was argued it would be

Table 1. Thermodynamic and transport properties of Freon 12 for the minimum and maximum working pressures on the rig (these limits are close to the two pressures used in the test programme). Critical point 4.11 MN/m^2 and 112°C; Boiling point at 0.1 MN/m^2 = −29.6°C

	Pressure (MN/m^2)	
	0·94	3.52
Saturation temperature (°C)	39.0	103.0
Liquid density (kg m^{-3})	1260.	865.
Vapour density (kg m^{-3})	53.5	283.0
Latent heat (kJ kg^{-1} °C^{-1})	129.0	55.2
Specific heat (kJ kg^{-1} °C^{-1})	1.01	1.85
Liquid dynamic viscosity (N s m^{-2})	241.0 × 10^{-6}	194.0 × 10^{-6}
Vapour dynamic viscosity (N s m^{-2})	12.9 × 10^{-6}	14.5 × 10^{-6}
Surface tension (N m^{-1})	7.37 × 10^{-3}	0.544 × 10^{-3}
Thermal conductivity (kW m^{-1} °C^{-1})	65.0 × 10^{-6}	30.0 × 10^{-6}

sufficient for our present purposes to demonstrate a similar pattern of behaviour between the two systems. The main effects of increasing pressure could then also be expected to be the same in the two systems.

In this particular situation it seemed likely that the gross flow patterns would largely determine the likelihood of dryout. The modelling rules were determined on this basis (Appendix 1), and indeed as will be seen in Sections 2.3 and 2.4, very similar dryout behaviour was experienced between the Freon 12 tests and the steam/water results reported by Lis & Strickland (1970). These same rules were then applied to determine the behaviour at the equivalent higher pressure of modern plant (Section 2.5).

2.2 *Freon* 12 *facility*

The Freon 12 facility was designed and constructed by Marchwood Engineering Laboratories. It operates over a range of temperatures and pressures lying close to the saturation values up to the critical point of dichlorodifluoromethane (CCl_2F_2—commonly referred to by its Dupont trade name of Freon 12), (table 1).

An outline flow chart of the system is shown in figure 1. The test section pressure normally lay close to that of the condenser which was controlled directly by a vapour by-pass from the boiler. An isolating valve at the exit to the test section could be used to raise the test section pressure well above saturation values, for special tests. In a Freon 12 system, this is a very convenient way of achieving sub-cooled conditions. It is made possible because the pressure rise across the main pump is a substantial proportion of the rig pressure.

Boiler pressure was controlled by a thyristor bank on the heaters, and the level was controlled using a capacitance probe. The more usual conduction devices could not be used because Freon 12 is non-conducting.

Superheat was controlled directly by a thermistor set in the vapour line. For very low vapour flow rates this was inadequate and so vapour was raised by pre-heating and flashing across the liquid flow control valve.

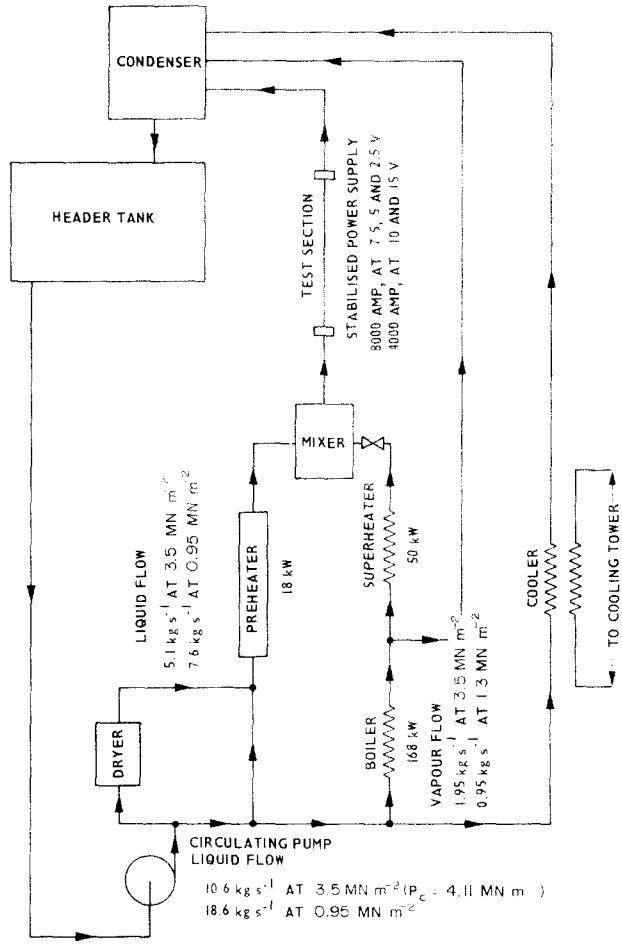

Figure 1. Simplified flow diagram for Freon 12.

Liquid and vapour flow rates were measured using a pair of turbine meters in each case, to an accuracy of $\pm\frac{1}{2}\%$. The inlet quality was calculated from the mixture of superheated vapour and sub-cooled liquid, on the basis of a heat balance, to an accuracy of $\pm\frac{1}{2}\%$. Heat losses were measured and allowed for but they were small corrections except for the vapour flashing runs when the higher corrections reduced the accuracy to $\frac{1}{2}\%$ point and 0.2% point for the high and low pressure runs respectively.

2.3 *Test section*

The Incoloy 800 test section was heated by passing an electric current through the tube walls between the electrodes shown in figure 2. The bends were not heated. The tube resistance was 0.00565 Ω at 21°C. The power was supplied by a voltage regulator, continuously variable up to 758 V and stabilized to $\pm 2\%$ for mains input variations of $\pm 10\%$.

The test section voltage/current requirement was met using a 60 kVA step down transformer with outputs as shown in figure 1.

Temperatures were measured using PVC covered chromel constantan thermocouples, spot-welded to the outside of the test section in groups of six as shown in figure 2. Any 24 of these could be connected via filter circuits with d.c. level adjustment to an u.v. recorder. S.M.I. Ltd. Z galvanometers were used with a natural frequency of 20 Hz adjusted to a sensitivity of 2°C per centimetre giving an overall accuracy for temperature measurement of $\pm\frac{1}{2}$°C.

2.4 *Low pressure tests*

Freon 12 tests were carried out at a pressure of 1 MN/m^2 absolute to correspond with the steam/water tests at 6.65 MN/m^2. The ranges of parameters covered at this pressure were: inner wall heat fluxes from 6 to 18.5 kW/m^2; mass velocities of 600 to 2200 kg/m^{2}s; inlet qualities from 3 to 85% for the low mass flow rates and from 3 to 17% for the high mass flow rates. The quality increase along the test section was typically about 2%.

Dry patches occurred along the top of the test section over a wide range of conditions. They were detected quite straightforwardly by the appearance of steady high top surface temperatures while the bottom temperatures remained low and steady. No problems were encountered in this and the presence of dry tube walls was decided by the overall behaviour of a number of galvanometer traces rather than by any single criterion. Figure 3 shows typical temperature distributions along the top of the test section plotted in terms of length to internal diameter ratio (L/D_i). It can be seen that the edges of the dry patches

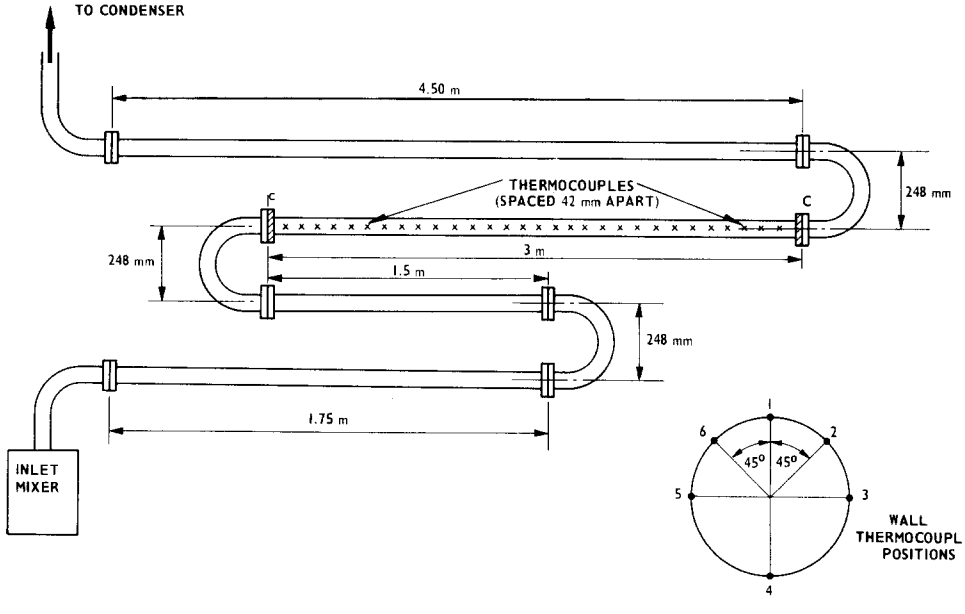

Figure 2. Serpentine test section showing power connections C–C and thermocouple positions.

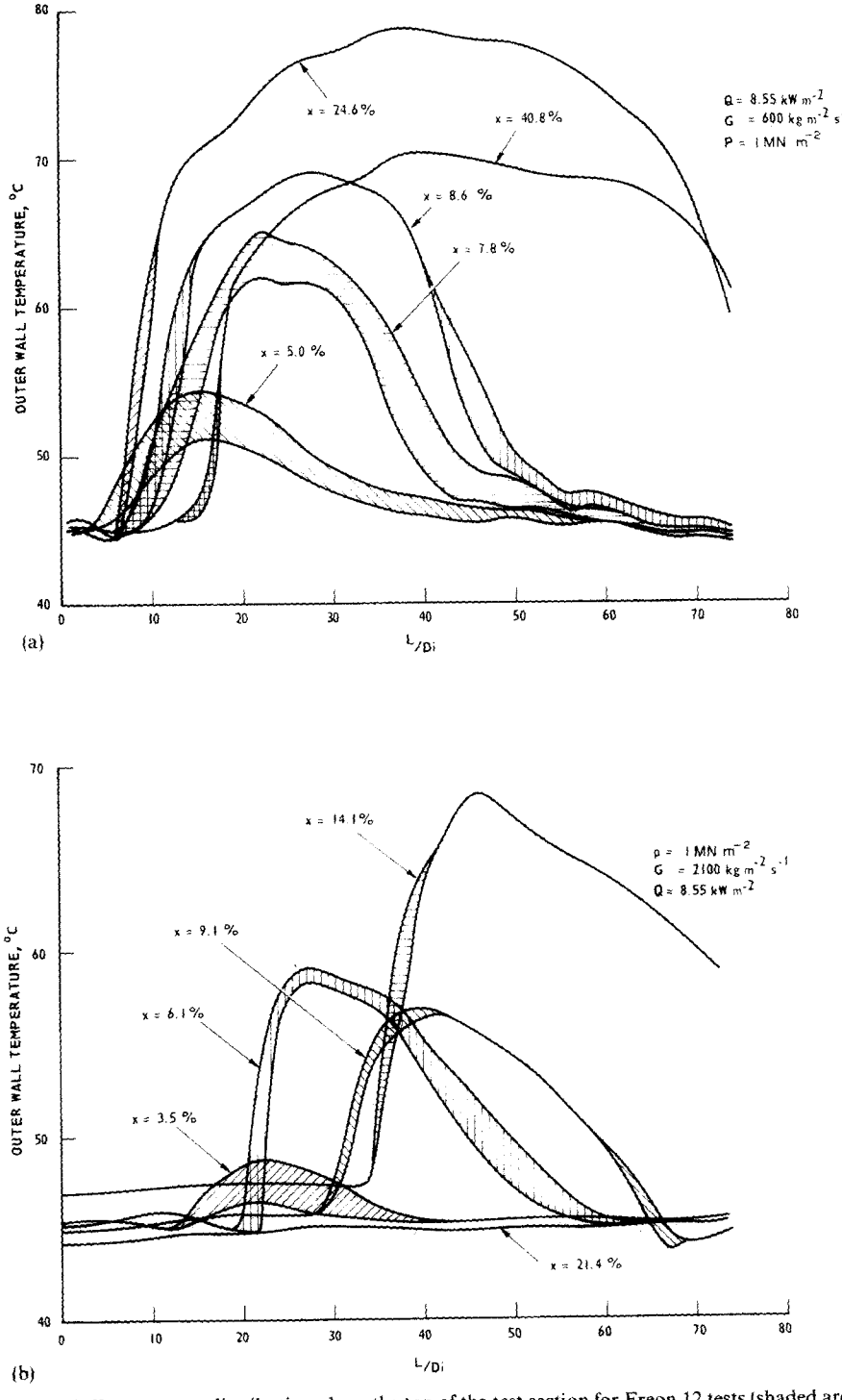

Figure 3. Temperature distribution along the top of the test section for Freon 12 tests (shaded areas show oscillating temperatures).

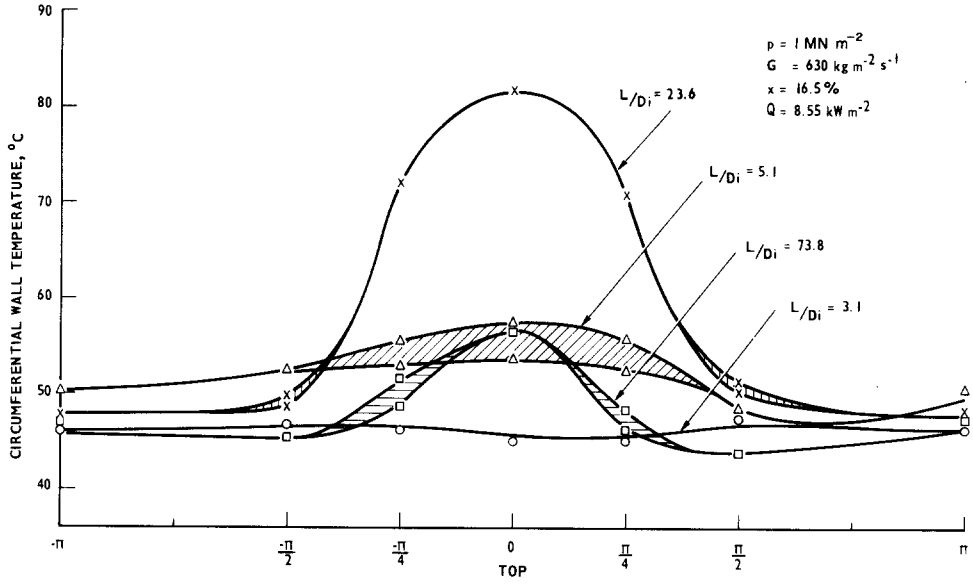

Figure 4. Circumferential temperature distribution for Freon 12 tests (shaded areas indicate oscillating temperatures).

were always bounded by short lengths of fluctuating temperature. Temperature fluctuations were never observed along the bottom of the tube. They remained low and steady throughout the tests. Along the top, the fluctuations generally varied in amplitude from about 2 to 6°C, but they were assumed to be oscillating if their amplitude was higher than $\frac{1}{2}$°C. The frequencies of oscillations varied from about 0.05 to 0.15 Hz for the larger amplitudes with higher frequencies of about 0.5 Hz of small amplitude, superimposed on these. Repeat tests showed that the upstream boundaries could be reproduced to an accuracy of $\pm 2L/D_i$ and the downstream boundaries to $\pm 10L/D_i$. Figure 4 shows typical circumferential temperature distributions.

The points on the tube where dry areas started and re-wetted were obtained for a range of conditions. When these were plotted for a particular value of pressure (P), mass velocity (G) and heat flux (Q), for a range of qualities (X), they produced curves like those in figure 5. The points where these curves cut any line parallel to the abscissa, show the extent of dryout on the test section for the conditions given. It may be seen that dry areas usually appeared first at qualities between about 5% and 10%. When the heat flux was low (e.g. $Q = 3.3\,\text{kW/m}^2$ in figure 5) the dry areas disappeared again at qualities of about 20 or 25%, and did not reappear as the quality increased up to the highest values measured ($\sim 70\%$). For higher heat fluxes, however, although dryout first appeared at the same low qualities, the subsequent behaviour was more complicated. It can be seen in figure 5, that when the heat flux was $8.6\,\text{kW/m}^2$, after the dry areas disappeared at about 35% quality, they re-appeared again at qualities above about 42%.

Generally, increasing the heat flux or decreasing the mass velocity caused the dry patch to move towards the inlet of the test section.

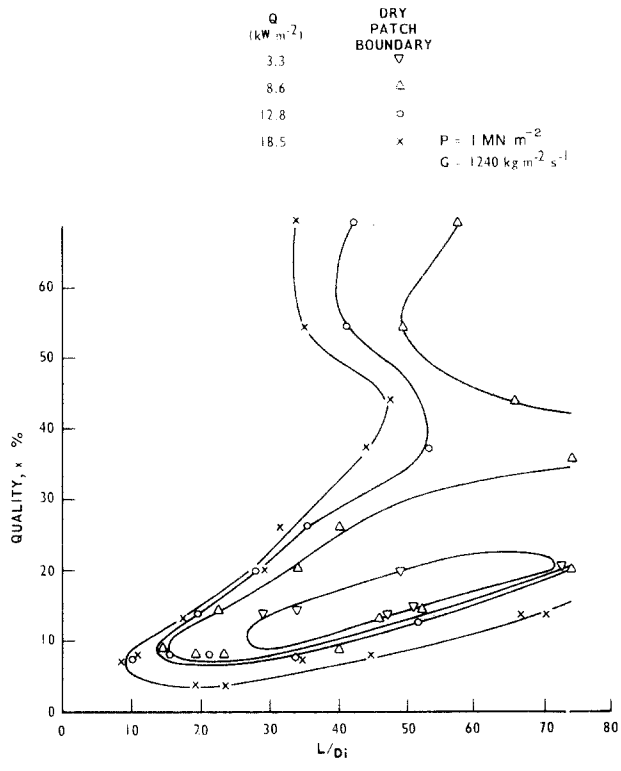

Figure 5. Effect of heat flux on the development of dry patches along the top of the test section for Freon 12 tests.

2.4 *Comparison of the Freon 12 tests with the Trawsfynydd steam/water results*

The low pressure Freon 12 results given above showed all the characteristics reported by Lis & Strickland (1970) for pressurized steam/water. Small dry patches appeared at low qualities of about 7% in just the same way. The re-wetting after dryout which occurred well before the end of the test section, was a particularly critical feature, appearing as it did in relatively few tests.

As quality was increased the dry patches retreated downstream, the leading edges moving almost identically in both systems (figure 6a), up to about 30% quality. The downstream edges in the Freon 12 tests extended rather further downstream but re-wetting would be much more sensitive to differences in physical properties, such as surface tension, and so this was not surprising.

For Trawsfynydd power station the range of interest stopped short at an outlet quality of about 40% and so most of the steam/water tests were not carried out at higher values for these conditions. A few steam/water tests were, however, and these (figure 7) did show the re-appearance of dryout at higher qualities like those for Freon 12 in figure 5. It is not clear therefore what significance to attach to the apparent differences shown in figure 6a

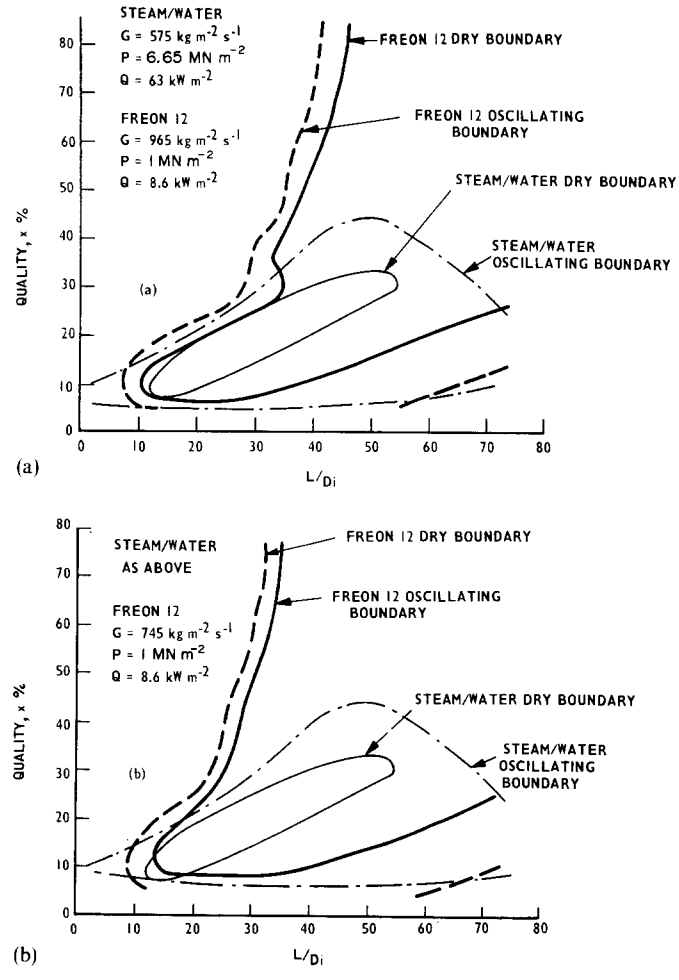

Figure 6. Comparison of oscillating and steady high temperature boundaries along the top of the test section between steam/water and Freon 12 based on (a) an equal volumes scaling rule; and (b) a "ρV^2" scaling rule.

at the higher qualities. The flows would have been well in the annular flow regime (see Appendix 2) and the simple modelling rules would not be expected to hold. Indeed, for accurate scaling it seems likely that scaling laws will need to be changed over a full quality range. Figure 6a was plotted on an equal volume basis. This was rather better than an equal "ρV^2" basis as shown in figure 6b, but the overall characteristics were the same for both.

Essentially, it was clear from the tests that up to qualities of about 40% the patterns of dryout were identical in both systems and this was quite sufficient for our purposes.

Lis & Strickland (1970) proposed a correlation for this type of dryout which had a

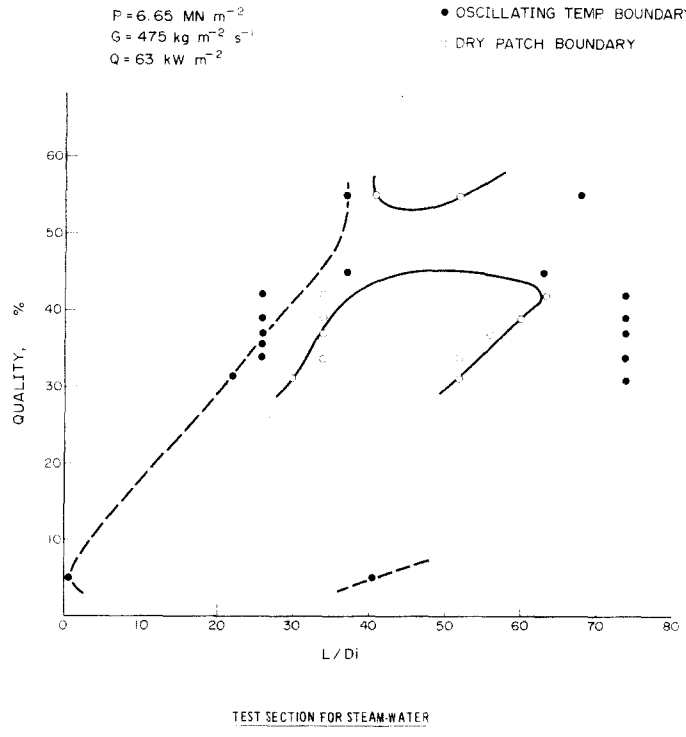

Figure 7. Development of oscillating temperatures and dry patches along the top of the test section for steam/water.

distinct change of slope depending on quality level. They suggested that the two slopes represented two flow regimes. It is interesting to note that all the steam/water conditions for the transition from dry to oscillating temperature could be fitted on a single straight line when plotted as in figure 8, where r is the internal tube radius, R the bend radius and g the acceleration due to gravity. Those Freon 12 tests which showed re-wetting at qualities above 30% also fell close to this line. There is no particular physical significance to the correlation but it makes the presence of two distinct regimes unlikely.

2.6 *High pressure tests*

These were carried out at 3.55 MN/m^2 in Freon 12 which was equivalent to about 18 MN/m^2 in steam/water. The other variables were as follows: mass flow velocities 1150 to 2850 kg/m^2 s; inlet qualities 14 to 68% for the low mass velocities and 8 to 34% for the high mass velocities, increasing typically by about 3%; heat fluxes from 6 to 18 kW/m^2.

For the range of conditions covered when dryout appeared the temperature profiles were all of the same form (figure 9). As in the low pressure tests, oscillating temperatures and dryout were detected soon after the bend. Unlike the low pressure tests, however, re-wetting did not take place. When quality was increased the start of the dry region moved towards the inlet and there was a fall in the level of steady high temperature.

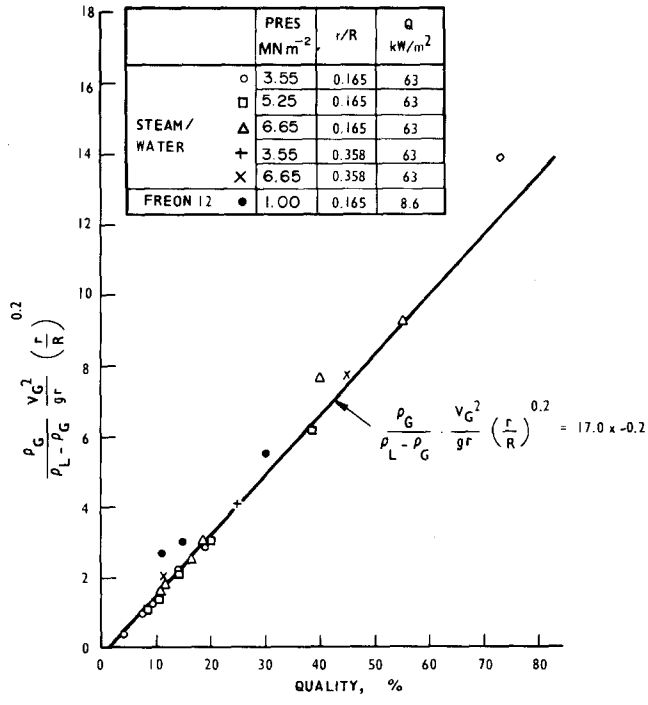

Figure 8. Correlation of the oscillating temperature boundary conditions for the Lis & Strickland (1970) steam/water tests and the Freon 12 results.

With high mass flow rates a region of fluctuating temperature appeared before any dry patch was formed. At the lowest flows and highest qualities (about 60%) the start of the dryout region retreated towards the exit with increasing quality. Heat flux did not have a big effect on the location of dryout, an increase from 6 to 18 kW/m^2 moving the start of dryout only $10L/D_i$ towards the inlet. The effect was slightly higher at high mass velocities.

To remove dryout completely for qualities above about 7%, the mass velocity had to be increased to 2530 kg/m^2 s.

It was clear from these results that the likelihood of dryout would not be reduced simply by increasing the reduced pressures to values of about 0.85. Indeed, the effect was to make dryout more likely and widespread.

3. AIR/WATER STUDIES

The first need was to describe the two phase flows in some detail in order to identify the types of flow which seemed particularly likely to lead to the dryout conditions described in Section 2 above.

An air/water system was used to take the fullest advantage this offered for flow visualization and to ease the instrumentation problems. An atmospheric steam/water facility was used also for some tests.

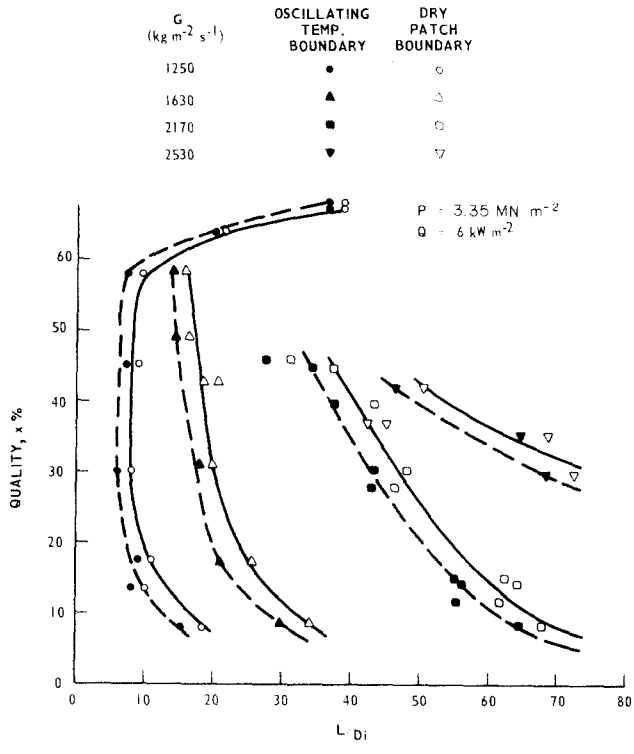

Figure 9. Development of oscillating and steady high temperature boundaries along the top of the test section for Freon 12.

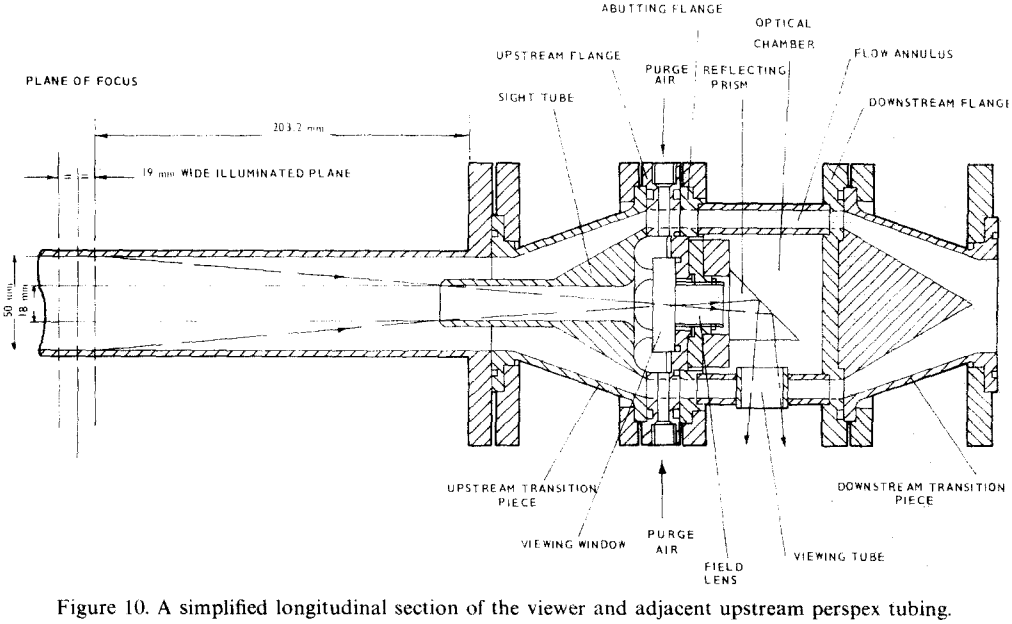

Figure 10. A simplified longitudinal section of the viewer and adjacent upstream perspex tubing.

3.1 *Flow regimes*

When liquid and vapour flow co-currently in a tube a wide range of complex flow patterns can be set up. Analysis indicates that they depend on an alarmingly high number of variables. Experience shows, however, that together with the flow rates it is the large difference in density between the liquid and vapour that is of overwhelming importance and it is possible to categorize the flows in terms of a relatively few broad types of flow pattern (e.g. Baker 1954; Schicht 1969; Hewitt & Roberts 1969; McMillan 1963; Al-Sheikh, Saunders & Brodkey 1970). It is possible to incorporate these in flow regime diagrams and these have proved to form a very useful framework in which to view two phase flows generally. Not many publications have dealt with horizontal flows and fewer with serpentines (Zahn 1964; Alves 1954).

Our studies have aimed at more detailed descriptions and in particular have concentrated on serpentine arrangements, using tubes of 19 mm, 31.8 mm and 50.8 mm bore tubes. High speed ciné techniques were necessary and as well as viewing through the walls of transparent test sections, a special viewer was used to look along the axes of the tubes (figure 10). This was based on a method first used by Hewitt & Roberts (1969) on vertical tubes. A wealth of detail was obtained in this way, but only the broad results can be described here.

The flow patterns have agreed surprisingly well with charts like that of Schicht (1969) (figure 11, where μ is dynamic viscosity and σ surface tension), though this was obtained largely from air and water studies and it is by no means certain how best to scale between different fluids. We tend to favour "ρV^2" modelling and this was shown to give good

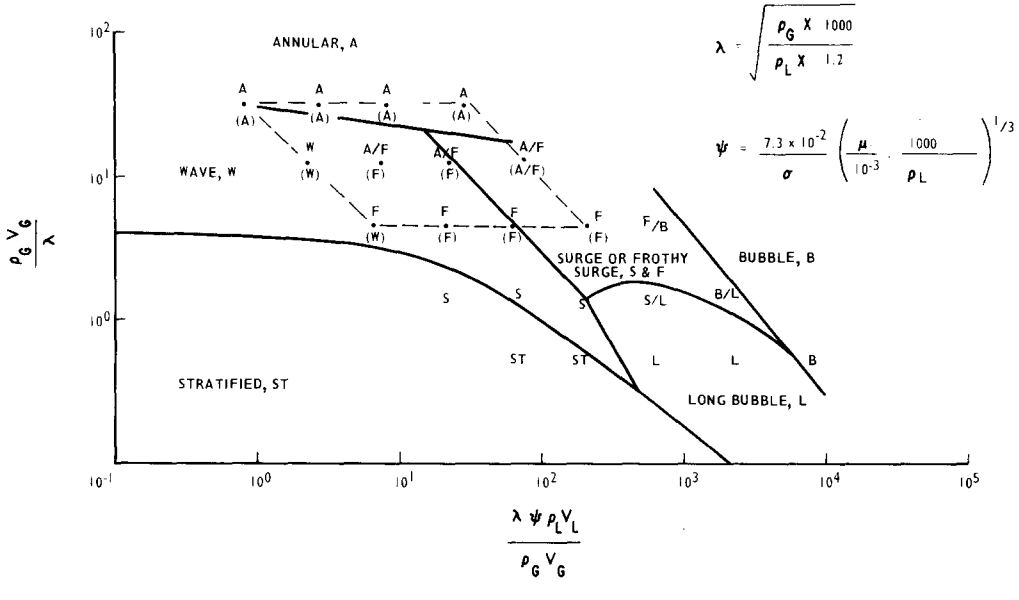

Figure 11. Flow regime chart by Schicht (1969). The flows observed by the authors are superimposed. Those obtained using the axial viewer are in parenthesis.

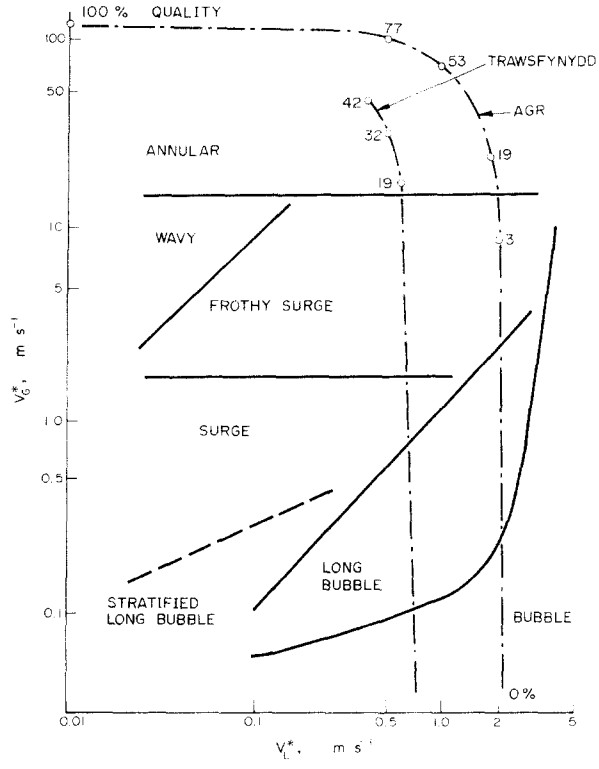

Figure 12. Flow regimes in serpentine evaporators, with power station operating curves.

agreement between air and water and pressurized steam/water tests by Hewitt & Roberts (1969), for vertical tubes.

Our serpentine results are represented by the flow regime chart given in figure 12. The flow regime descriptions are given in Appendix 2. The chart was derived from visualization tests on the 50.8 mm bore tubes. Visually, the flow regimes did not appear to be sensitive to diameter for the values examined. However, the frothy surge/annular flow transition is an important one and this was checked by film thickness measurements. These indicated that the boundary moved from V_G^* values of 15 m s^{-1} at 19 mm bore to 20 m s^{-1} at 50.8 mm bore.

The chart also shows operating curves for Trawsfynydd power station which was an early Magnox design and for an Advanced Gas Cooled Reactor station. These curves may be obtained very simply. For any boiler,

$$V_G = \rho_L/\rho_G(V_{LO} - V_L)$$

where V_G and V_L are the superficial velocities (G/p) and ρ_G and ρ_L are the densities of the vapour and liquid respectively. V_{LO} is the superficial velocity of the liquid for zero quality.

Modelling on the basis of "ρV^2" terms

$$V_L^* = V_L\sqrt{\frac{\rho_L}{\rho_L^*}}$$

where the superscript * represents the "modelled value", and

$$V_G^* = V_G \sqrt{\frac{\rho_G}{\rho_G^*}}.$$

Therefore

$$V_G^* = V_{LO}^* \sqrt{\frac{\rho_L \rho_L^*}{\rho_G \rho_G^*}} \left(1 - \frac{V_L^*}{V_{LO}^*}\right).$$

Trawsfynydd being a re-circulating drum boiler, has a maximum quality of about 40%. All the current AGR's are "once-through" designs.

At low qualities, certainly below 5% or so, it is very important to get the gas and liquid volumes the same in both systems. This requires changes in the relationships given above but the curves would not look very different on the diagram.

For dryout conditions in Trawsfynydd power station the flows fell mainly in the "frothy surge" regime and so this type of flow was given most attention.

3.2 *Frothy surge flows*

As may be seen from Appendix 2, this region on the chart is characterized by trains of frothy liquid surges. They have been noted by others (Schicht 1969, etc.) and they are recognized as being important in determining pressure drops (Greskovich & Shrier 1971; Vermeulen & Ryan 1971, etc.). Looking at this type of flow rather differently we have proposed that the surges are the only mechanisms supplying liquid to the top surface and that in between them the liquid film is free to drain without replenishment. The liquid is mainly transported in the surges and there is a strong dependency of surge frequency on liquid flow rate. Vapour flow rate is also important and so the liquid transported by each surge must vary considerably. The velocities of the surges are usually well below the combined superficial velocities of the liquid and vapour and clearly they do not then block the tube. Measurements of liquid film thickness within the surge indicate values of a few millimetres. The whole process is well represented by figure 13 which shows liquid

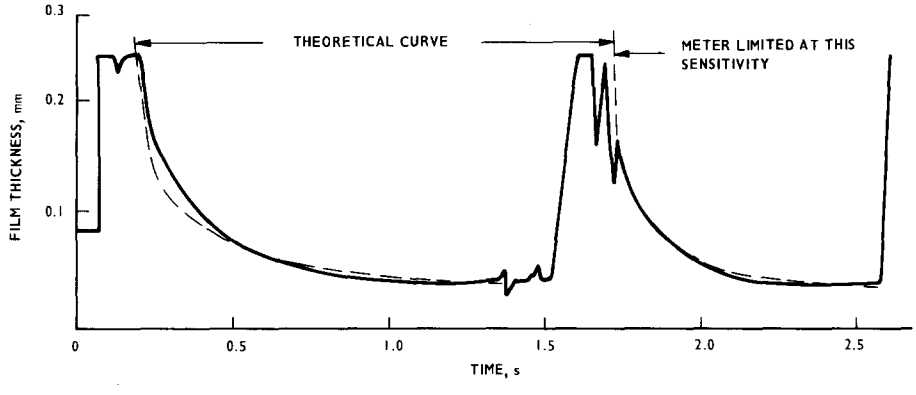

Figure 13. Typical draining curves obtained in surge flow.

film thickness measurements made along the top surface using an instrument specially designed for this purpose (Coney 1973).

A theory has been proposed completely describing the build-up of a liquid film along the top surface in a surge and also the draining and evaporation behind it. Film thickness measurements made for a wide range of flow rates in the air/water facility confirmed the analysis (Coney 1974). Good agreement was also obtained by the authors (figure 13) in an atmospheric steam/water facility. This was a 6 pass serpentine arrangement of 50 mm bore tubes in which one pass was an electrically heated Incoloy test section, instrumented with film thickness probes like those described by Coney (1974) for air/water measurements.

It may be seen that when the interval between surges is longer than the time taken for the liquid film to drain and evaporate away, the surface will dry out. If the interval is particularly long the surface may not be re-wetted by the following surge. This seems to be most likely at the higher vapour and lower liquid flow rates near the annular flow transition when the splashing within a surge appears to be a minimum.

The effect of increased pressure in the Freon 12 tests can now be understood. Figure 14 shows how the lower latent heat (H_{VL}) and viscosity at the higher saturation pressure gave more rapid draining and evaporation rates. This figure also shows draining curves for steam/water and Freon 12 at the Traswfynydd conditions. It was encouraging that they turned out to be so similar.

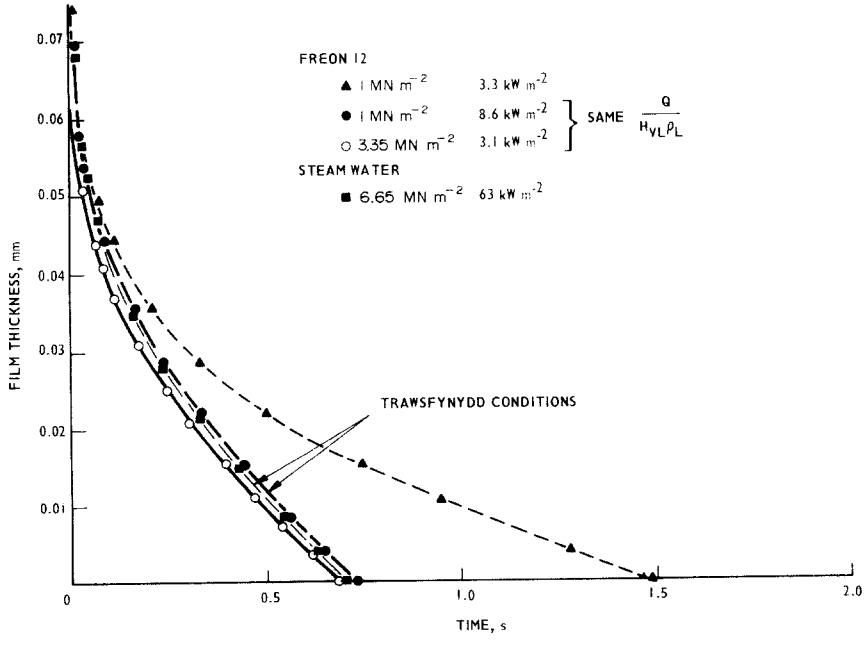

Figure 14. The effect of pressure on draining curves in Freon 12.

3.3 *Application to dryout assessment*

The draining theory enables a dryout time to be calculated after the passing of a frothy surge in any fluid. However, to obtain the likelihood of dryout it is necessary to know the complete distribution of surge intervals. Correlations have been published for mean surge frequency (Vermeulen & Ryan 1971; Gregory & Scott 1969; Greskovitch & Shrier 1972; Hubbard 1965; Kordyban & Ranov 1963, etc.), but none for surge intervals. We have therefore been measuring surge intervals in our own facilities. These show a wide distribution about the mean and this cannot be ignored for it is clearly the longest intervals which are most likely to cause dryout. In addition the distribution appears to be a function of diameter below about 50 mm bore, the most important effect being that the longest intervals are cut-off as the diameter is reduced, particularly at low liquid flows.

An assessment of dryout is therefore not a simple matter and it is not appropriate to describe this work, which is still continuing, here. An indication of the progress being made can however be given.

It has been easiest to measure surge intervals in the air/water and atmospheric steam/water facilities. As an interim measure these data are being scaled empirically for application to pressurized steam/water facilities. Greskovitch & Shrier (1972) suggested that the effect of physical properties on surge frequency was small. Intuitively, ρV^2 terms

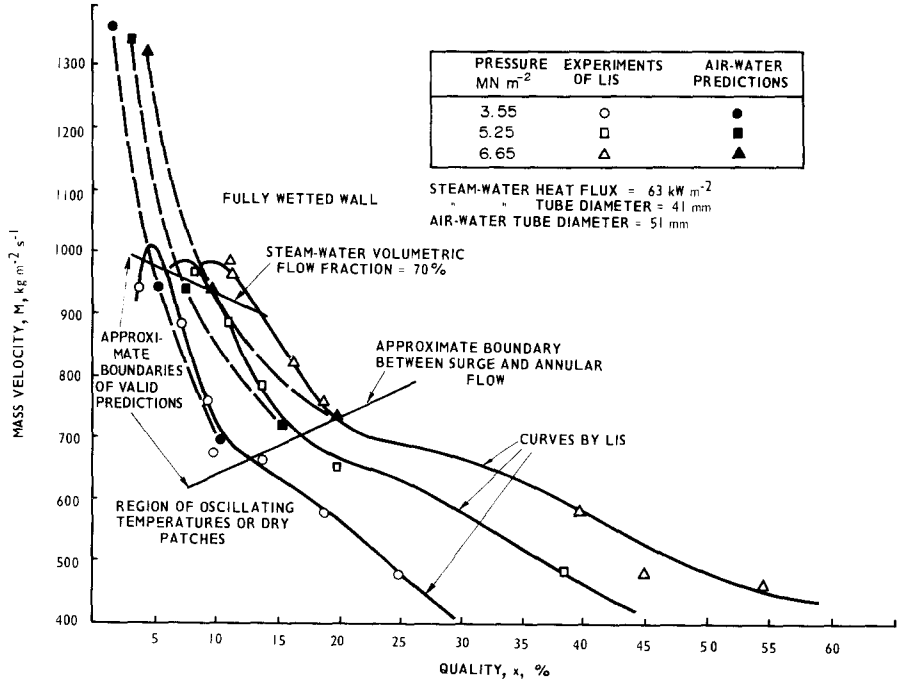

Figure 15. Comparison of air/water predictions (Coney 1974) with the data of Lis & Strickland (1970) at three different pressures.

would be expected to be important and surge frequency data between our air/water and steam/water facilities have agreed well on this basis. Scaling on this basis has been adopted provisionally and very good predictions of the Lis & Strickland (1970) dryout boundaries have been made (figure 15). Dryout in Freon 12 was under-predicted on this basis and Froude number modelling as suggested by Gregory & Scott (1969) would have been better. Surge intervals will be measured directly in Freon 12 using a probe designed for this purpose (Benn 1972) to give a proper indication of the effect of physical properties.

The method is currently being developed to estimate the duration and frequency of the dryout periods. This is needed in particular for studies on stress corrosion, but it may also be very important for determining which types of dryout give rise to on-load corrosion.

4. CONCLUSIONS

4.1 Dryout which has given rise to rapid on-load corrosion failures in serpentine evaporators is likely at intermediate qualities for a wide range of flow rates and pressures, at very much lower heat fluxes than previously experienced in vertical tubes.

4.2 Types of two phase flow which are particularly likely to dryout have been identified and labelled "surge-flow" and "frothy surge flow".

4.3 In these flows the top surfaces of tubes are washed intermittently by waves or plugs of frothy liquid and between these the liquid film drains and evaporates from the top surface without replenishment.

4.4 A theory has been proposed which correctly predicts the draining behind a frothy surge (Coney 1974).

4.5 The dryout boundaries in a pressurized steam/water facility were correctly predicted using the draining theory to calculate a dryout time and data on surge intervals obtained in an air/water facility scaled on the basis of a "ρV^2" modelling assumption.

Acknowledgements—Thanks are due to Mr. C. E. Hopley for his help in the design of the axial viewer and the associated experiments also for assistance with the Freon 12 tests together with Mr. P. Hanks and Mr. J. Wyrill.

The C.E.R.L. photographic section carried out all the photographic work.

In particular acknowledgement is made to Mr. M. W. E. Coney for the theory used in the dryout assessment.

The work was carried out at the Central Electricity Research Laboratories, Leatherhead and the paper is published by permission of the Central Electricity Generation Board.

REFERENCES

AHMAD, S. Y. 1973 Fluid to fluid modelling of critical heat flux: A compensated distortion model, *Int. J. Heat Mass Transfer* **16**, 641–662.

AL-SHEIKH, J. N., SAUNDERS, D. E. & BRODKEY, R. S. 1970 Prediction of flow patterns in horizontal two-phase pipe flow, *Can. J. Chem. Engng* **48**, 21–29.

ALVES, G. E. 1954 Cocurrent liquid–gas flow in a pipe-line contactor, *Chem. Engng. Progr.* **50**, 449–456.

BAKER, O. 1954 Simultaneous flow of oil and gas, *Oil & Gas J.* **53**, 185–215.

BARNETT, P. G. 1964 An Experimental Investigation to Determine the Scaling of Forced Convection Boiling Heat Transfer. AEEW-R, 363. U.K.A.E.A.

BARNETT, P. G. 1963 The Scaling of Forced Convection Boiling Heat Transfer. AEEW-R134, U.K.A.E.A.

BENN, D. N. 1972 An Experimental Capacitance Liquid Film Thickness Monitor. AERE-R 7155.

CONEY, M. W. E. 1973 The theory and application of conductance probes for the measurement of liquid film thickness in two-phase flow, *J. Phy. E: Sci. Instrum.* **6**, 903–910.

CONEY, M. W. E. 1974 The analysis of a mechanism of liquid replenishment and draining in horizontal two-phase flow, *Int. J. Multiphase Flow* **1**, 647–669.

GARNSEY, R., HEARN, B. & MANN, G. M. W. 1972 *J. Br. Nucl. Energy Soc.* **11**, 75–70.

GREGORY, G. A. & SCOTT, D. S. 1969 Correlation of liquid slug velocity and frequency in horizontal cocurrent gas–liquid slug flow, *A.I.Ch.E. J.* **15**, 933–935.

GRESKOVICH, E. J. & SHRIER, A. L. 1971 Pressure drop and hold-up in horizontal slug flow, *A.I.Ch.E. J.* **17**, 1214–1219.

GRESKOVICH, E. J. & SHRIER, A. L. 1972 Slug frequency in horizontal gas–liquid slug flow, *Ind. Engng. Chem. Process. Des. Develop.* **11**, 317–318.

HEWITT, G. F. & ROBERTS, D. N. 1969 Studies of Two-phase Flow Patterns by Simultaneous X-Ray and Flash Photography. AERE-M2159, U.K.A.E.A.

HEWITT, G. F. & ROBERTS, D. N. 1969 Investigation of Interfacial Phenomena in Annular Two-Phase Flow by Means of the Axial View Technique. AERE-R6070.

HUBBARD, M. G. 1965 Analysis of Horizontal Gas–Liquid Slug Flow. Ph.D. Thesis, University of Houston, Texas.

KORDYBAN, E. S. & RANOV, T. 1963 Experimental Study of the Mechanism of Two-Phase Slug Flow in Horizontal Tubes, Multiphase Flow Symp., Winter Annual Meeting of ASME, Phila. P.A., 17–22 November.

LIS, J. & STRICKLAND, J. A. 1970 Local Variations of Heat Transfer in a Horizontal Steam Evaporator Tube, *4th Int. Heat Transfer Conf. Paris,* Vol. 5, B4.6.

LUNN, D. C. F. & HARVEY, J. 1970 Corrosion at Trawsfynydd, *J. Energy* **20**, 189–191.

MCMILLAN, H. K. 1963 A Study of Flow Patterns and Pressure Drop in Horizontal Two-Phase Flow. Ph.D. Thesis, Purdue University, Iniv. Microfilm, Ann Arbor, Michigan, No. 16257.

SCHICHT, H. H. 1969 Flow patterns for an adiabatic two-phase flow of water and air within a horizontal tube, *Verfahrenstechnik* **3**, 153–161.

VERMEULEN, L. R. & RYAN, J. T. 1971 Two phase slug flow in horizontal and inclined tubes, *Can. J. Chem. Engng* **49**, 195–201.

ZAHN, W. R. 1964 A Visual Study of Two-Phase Flow while Evaporating in Horizontal Tubes. ASME Paper 63-WA-166.

APPENDIX 1

Modelling rules

Pressure: This was chosen to give the same liquid to vapour density ratio in both systems. It has been a common choice from the earliest days (Barnett 1963, 1964).

Flow rate: A range of liquid and vapour flow rates was chosen to include modelling both in terms of equal volume flow rates and in terms of equal "ρV^2" values.

Heat flux: This was chosen to evaporate the same volume rate of liquid in both systems. Because of the pressure rule this also gave the same generation rate of vapour, which can be a very important requirement when a significant volume of vapour is generated.

It is interesting to note that later work by other authors, aimed at more precise scaling would have given very similar results to those of the above modelling rules. For example, the "compensated distortion" model of Ahmad (1973) based on a comprehensive analysis of two phase modelling gave precisely the same numerical values for the scaling factors for the lower pressure tests. It was only when the critical point was being approached and the surface tension for Freon 12 was dropping to much lower values than the pressurized water that significantly different scaling factors were calculated.

APPENDIX 2

Flow regime definitions for horizontal flows

Some of the terms used below (*) are not the same as those generally used. It was with some reluctance that these were introduced. It became necessary, firstly, because of the confusion and inconsistencies in the current terminology and secondly to represent more meaningful divisions, not previously highlighted.

Bubble flow (*B*), consists mainly of liquid with vapour in the form of small bubbles, dispersed throughout the liquid. The greatest dimension of any bubble will be less than the tube diameter.

Long bubble flow (*LB*), consists of discrete vapour bubbles of greatest dimension at least that of the tube diameter. Smaller bubbles may also be present. This is often called "plug flow".

Stratified flow (*St*), occurs when all the liquid has settled to the bottom of the tube. The surface will be smooth with perhaps gentle undulating waves. There will be no liquid entrained in the vapour. This is not a stable condition in a serpentine.

Wavy flow (*W*), is sometimes said to be similar to stratified flow but the depth of liquid is much shallower and the liquid surface is very disturbed. It will look very similar to annular flow but with a continuously dry top surface.

**Surge flow* (*S*), is basically a stratified flow with a series of waves or liquid plugs "surging" along the tube. The plugs and waves may contain small vapour bubbles. Surge flow could also be described as an extreme case of long bubble flow where the bubbles are so long that attention is focussed on the water between them. It would be commonly called "slug flow".

**Frothy surge flow* (*F*), looks like a wavy flow with a series of very frothy waves or plugs surging along the tube. The frothy surges may be a metre long and although they contain a great deal of splashing and liquid entrainment, producing liquid film thicknesses usually in excess of 2 mm along the top of the tube, they are largely hollow. The common practice of including this in slug flow is quite misleading.

Annular flow (*A*), is characterized by a continuous film of liquid on the walls of the tube, with droplets of liquid distributed throughout the vapour core. The liquid film will

be very disturbed, and large waves may be present with a lot of splashing and liquid entrainment associated with them. At the highest liquid flows, quite large disturbances may be present but these will never block the tube. The boundary between frothy surge flow and annular flow is difficult to define, visually. Measurement shows that liquid films appear to be maintained continuously along the upper surfaces for vapour superficial velocities between about 15 and 20 m s^{-1} for tube diameters between 19 mm and 50 mm, for atmospheric steam water and air/water tests.

Dispersed flow, occurs when the liquid films in annular flows are breaking up into rivulets and detaching from the walls. More liquid will be entrained in the vapour than is attached to the walls.

Résumé—Des ruptures par corrosion dans les évaporateurs de centrales de puissance peuvent resulter de phénomènes d'assechement de la génératrice supérieure des tubes qui sont disposés en serpentin.

On montre que ce type d'assèchement peut se produire à des qualités intermédiaires dans une large gamme de débits et de pressions, pour des flux de chaleur inférieurs à ceux qui provoqueraient l'assèchement dans des conduites verticales.

On a identifié un type d'écqulement, appelé ici "écoulement par vagues", comme étant particulièrement susceptible de provoquer des assèchements. En effet, avec cet écoulement, les parois supérieures ne sont alimentées un liquide que par intermittence, par des vagues ou des bouchons de liquide écumant.

On donne une méthode permettant d'évaluer la probabilité d'assèchement dans les conditions des écoulements par vagues. La méthode permet le calcul correct des limites d'assèchement dans un système pressurisé eau vapeur.

Auszug—Wasserseitige Korrosionsausfaelle von Kraftwerksverdampfern waehrend des Betriebes wurden durch Trockenwerden der Scheiteloberflaechen von Rohren in Schlangenanordnung verursacht. Es wird gezeigt, dass ein solches Trockenwerden, bei mittleren Dampfgehalten in einem weiten Bereich von Durchflussgeschwindigkeiten und Druecken, bei Waermestroemen vorkommt, die weit geringer sind als in vertikalen Rohren. Eine Stroemungsform, hier "surge flow (Stoss-Stroemung)" genannt, wurde als besonders anfaellig fuer Trockenwerden identifiziert, da bei ihr die Scheitelflachen nur mit Unterbrechungen durch Wellen oder Pfropfen schaumiger Fluessigkeit benetzt werden. Es wird eine Methode entwickelt, um die Wahrscheinlichkeit eines Trockenwerdens unter Stoss-Stroemungsbedingungen abzuschaetzen. Sie ergibt eine richrige Vorhersage der Grenzen des Trockenwerdens in einer Dampf/Wasser Druckanlage.

Резюме—Коррозионное разрушение под нагрузкой на водяной стороне и спарителей электрических станций проистекает из пересыхания вдоль верхней поверхности труб змеевиковых устройств.

Показано, что данное пересыхание может возникать при промежуточном (переходном) режиме в слишком широком диапазоне скоростей потока и давлений, для горячих потоков значительно менее, чем в вертикальных трубах.

Тип течения, которых назван в работе потоком валов, определен как могущий с большой вероятностью привести к пересыханию, ввиду того что верхние поверхности смачиваются не иначе, как попеременно волнами и хлопьями вспененной жидкости.

Метод развит для оценки вероятности высыхания в услових течения валов и позволяет правильно предскаазть границы пересыхания в пароводяном оборудовании, находящемся под давлением.